ANL-6664

Argonne National Laboratory

TESTING OF CONTAINMENT CAPABILITIES OF REINFORCED CONCRETE-SHIELDED ENCLOSURES

by

S. H. Fistedis, A. H. Heineman,
and
M. J. Janicke

ANL-6664
Reactor Technology
(TID-4500, 19th Ed.)
AEC Research and
Development Report

ARGONNE NATIONAL LABORATORY
9700 South Cass Avenue
Argonne, Illinois

TESTING OF CONTAINMENT CAPABILITIES OF REINFORCED CONCRETE-SHIELDED ENCLOSURES

by

S. H. Fistedis, A. H. Heineman, and M. J. Janicke

Reactor Engineering Division

March 1963

Operated by The University of Chicago
under
Contract W-31-109-eng-38
with the
U. S. Atomic Energy Commission

Table II — GEOMETRIC PROPERTIES OF SECTIONS AND CALCULATED REACTIONS, MOMENTS, STRESSES, AND STRAINS FOR 10 PSIG PRESSURE

	GAGE NO.*	1	2	3	4	5	6	7	9	11	13	14	16	17	18	19	20	21	22	23	24	25	26	27	28	29	30	31	32	33	34	35	36	38	39	40	41	42	43	44
P_1 P_2 P	P, lb	16,280	16,280	6,950	6,950	16,280	16,280	7,240	16,280	10,420	16,280	16,280	6,950	16,280	16,280	7,240	7,240	16,280	16,280	6,950	6,950	16,280	16,280	7,240	7,240	11,190	11,190	7,370	7,370	11,190	11,190	7,600	7,600	11,190	7,370	7,370	11,190	11,190	7,600	7,600
STRESSES - IN PLANE OF FRAMES	A, in.^{2}	596.6	596.6	740.6	740.6	596.6	596.6	595.6	596.6	596.6	596.6	596.6	740.6	596.6	596.6	596.6	596.6	596.6	596.6	740.6	740.6	596.6	596.6	596.6	596.6	596.6	596.6	740.6	740.6	596.6	596.6	596.6	596.6	596.6	740.6	740.6	596.6	596.6	596.6	596.6
	P/A, lb/in.^{2}	27.3	27.3	9.4	9.4	27.3	27.3	12.1	27.3	17.5	27.3	27.3	9.4	27.3	27.3	12.1	12.1	27.3	27.3	9.4	9.4	27.3	27.3	12.1	12.1	18.8	18.8	10.0	10.0	18.8	18.8	12.7	12.7	18.8	10.0	10.0	18.8	18.8	12.7	12.7
	$M/10^3$, lb-in.	+386	-445	+209	-300	+417	-582	+190.3	-622	-344	+582	-687	-450	+550	-550	+358	-358	-659	+665	-451	+455	-644	+673	-456	+452	+337	-318	+88.2	-110.0	+295	-282	+201	-105.2	+350	-515	+518	-347	+354	-481	+488
	C, in.	20	20	26	26	20	20	20	20	20	20	20	26	20	20	20	20	20	20	26	26	20	20	20	20	20	20	26	26	20	20	20	20	20	26	26	20	20	20	20
	I, in.^{4}	118,400	118,400	229,350	229,350	118,400	118,400	118,400	118,400	118,400	118,400	118,400	229,350	118,400	118,400	118,400	118,400	118,400	118,400	229,350	229,350	118,400	118,400	118,400	118,400	118,400	118,400	229,350	229,350	118,400	118,400	118,400	118,400	118,400	229,350	229,350	118,400	118,400	118,400	118,400
	S, in.^{3}	5,920	5,920	8,820	8,820	5,920	5,920	5,920	5,920	5,920	5,920	5,920	8,820	5,920	5,920	5,920	5,920	5,920	5,920	8,820	8,820	5,920	5,920	5,920	5,920	5,920	5,920	8,820	8,820	5,920	5,920	5,920	5,920	5,920	8,820	8,820	5,920	5,920	5,920	5,920
	M/S, lb/in.^{2}	+65.2	-75.1	+23.6	-34.0	+70.4	-98.3	+32.1	-105.0	-58.1	+98.3	-116.0	-51.0	+92.9	-92.9	+60.4	-60.4	-111.3	+112.3	-51.1	+51.5	-108.7	+113.6	-77.0	+76.3	+56.9	-53.7	+10.0	-12.4	+49.8	-47.6	+33.9	-17.7	+59.1	-58.3	+58.7	-58.6	+59.7	-81.2	+82.4
	$\sigma_1 = \frac{P}{A} + \frac{M}{S}$, lb/in.^{2}	92.5	—	33.0	—	97.7	—	44.2	—	—	125.6	—	—	120.2	—	72.5	—	—	139.6	—	60.9	—	140.9	—	88.4	75.7	—	20.0	—	68.6	—	46.6	—	77.9	—	68.7	—	78.5	—	95.1
	$\sigma_2 = \frac{P}{A} - \frac{M}{S}$, lb/in.^{2}	—	47.8	—	24.6	—	71.0	—	77.7	40.6	—	88.7	41.6	—	65.6	—	48.3	84.0	—	41.7	—	81.4	—	64.9	—	—	34.9	—	2.4	—	28.8	—	5.0	—	48.3	—	39.8	—	68.5	—
	σ_u, lb/in.^{2}	+92.5	-47.8	+33.0	-24.6	+97.7	-71.0	+44.2	-77.7	-40.6	+125.6	-88.7	-41.6	+120.2	-65.6	+72.5	-48.3	-84.0	+139.6	-41.7	+60.9	-81.4	+140.9	-64.9	+88.4	+75.7	-34.9	+20.0	-2.4	+68.6	-28.8	+46.6	-5.0	+77.9	-48.3	+68.7	-39.8	+78.5	-68.5	+95.1
STRESSES - 90° TO PLANE OF FRAMES	—																																							
	P', lb	11,190	11,190	7,370	7,370	11,190	11,190	7,600	10,420	16,280	11,190	11,190	7,370	11,190	11,190	7,600	7,600	11,190	11,190	7,370	7,370	11,190	11,190	7,600	7,600	16,280	16,280	6,950	6,950	16,280	16,280	7,240	7,240	16,280	6,950	6,950	16,280	16,280	7,240	7,240
	P'/A, lb/in.^{2}	18.8	18.8	10.0	10.0	18.8	18.8	12.7	17.4	27.3	18.8	18.8	10.0	18.8	18.8	12.7	12.7	18.8	18.8	10.0	10.0	18.8	18.8	12.7	12.7	27.3	27.3	9.4	9.4	27.3	27.3	12.1	12.1	27.3	9.4	9.4	27.3	27.3	12.1	12.1
	$M'/10^3$, lb-in.	—	—	—	—	—	—	—	-346	-626	—	—	—	—	—	—	—	-368	+376	-515	+521	-360	+358	-491	+477	—	—	—	—	—	—	—	—	+682	-453	+461	-677	+661	-460	+454
	M'/S, lb/in.^{2}	—	—	—	—	—	—	—	-58.4	-105.7	—	—	—	—	—	—	—	-62.2	+63.5	-58.4	+59.1	-60.8	+60.5	-82.9	+80.6	—	—	—	—	—	—	—	—	+115.2	-51.4	+52.3	-114.4	+111.7	-77.7	+76.7
	$\sigma'_1 = \frac{P'}{A} + \frac{M'}{S}$, lb/in.^{2}	18.8	18.8	10.0	10.0	18.8	18.8	12.7	—	—	18.8	18.8	10.0	18.8	18.8	12.7	12.7	—	82.3	—	69.1	—	79.3	—	93.3	27.3	27.3	9.4	9.4	27.3	27.3	12.1	12.1	142.5	—	61.7	—	139.0	—	88.8
	$\sigma'_2 = \frac{P'}{A} - \frac{M'}{S}$, lb/in.^{2}	—	—	—	—	—	—	—	41.0	78.4	—	—	—	—	—	—	—	43.4	—	48.4	—	42.0	—	70.2	—	—	—	—	—	—	—	—	—	—	42.0	—	87.1	—	65.6	—
	σ_v, lb/in.^{2}	18.8	18.8	10.0	10.0	18.8	18.8	12.7	-41.0	-78.4	18.8	18.8	10.0	18.8	18.8	12.7	12.7	-43.4	82.3	-48.4	69.1	-42.0	79.3	-70.2	93.3	27.3	27.3	9.4	9.4	27.3	27.3	12.1	12.1	142.5	-42.0	61.7	-87.1	139.0	-65.6	88.8
STRAINS	—																																							
	$\mu^\dagger \sigma_v$	3.8	3.8	2.0	2.0	3.8	3.8	2.5	-8.2	-15.7	3.8	3.8	2.0	3.8	3.8	2.5	2.5	-8.7	16.5	-9.7	13.8	-8.4	15.9	-14.0	18.7	5.5	5.5	1.9	1.9	5.5	5.5	2.4	2.4	28.5	-8.4	12.3	-17.4	27.8	-13.1	17.8
	$\sigma_u - \mu\sigma_v$	+88.7	-51.6	+31.0	-26.6	+93.9	-74.8	+41.7	-69.5	-24.9	+121.8	-92.5	-43.6	+116.4	-69.4	+70.0	-50.8	-75.3	+123.1	-38.0	+47.1	-73.4	+125.0	-50.9	+69.7	+70.2	-40.4	+18.1	-4.3	+63.1	-34.3	+44.2	-7.4	+49.4	-39.9	+56.4	-22.4	+50.7	-55.4	+77.3
	$\varepsilon_u = \frac{1}{E}\left(\sigma_u - \mu\sigma_v\right)$	+22.2	-12.9	+7.8	-6.7	+23.5	-18.7	+10.4	-17.4	-6.2	+30.5	-23.1	-10.9	+29.1	-17.4	+17.5	-12.7	-18.8	+30.8	-8.0	+11.8	-18.4	+31.3	-12.7	+17.4	+17.6	-10.1	+4.5	-1.1	+15.8	-8.6	+11.1	-1.9	+12.4	-10.0	+14.1	-5.6	+12.7	-13.9	+19.3

*Gages numbered 8, 10, 12, 15, and 37 were defective.

† μ = 0.20

‡ $E = 4 \times 10^6$

TABLE OF CONTENTS

LIST OF FIGURES

LIST OF FIGURES

LIST OF TABLES

TESTING OF CONTAINMENT CAPABILITIES OF REINFORCED CONCRETE-SHIELDED ENCLOSURES

by

S. H. Fistedis, A. H. Heineman, and M. J. Janicke

ABSTRACT

A reinforced concrete-shielded enclosure intended to contain nuclear reactor experiments was subjected to internal pressures up to 10 psig. The strains in reinforcing steel were measured with strain gages at critical locations for each pressure increment. These strains were compared with calculated strains; good agreement was found if the appropriate stress-concentration factors are applied at locations near re-entrant corners and wall openings.

Leakage-rate tests were performed to disclose the ability of an ordinary thick-walled concrete cell to contain compressed gases. Observed leak rates are given for the two twin cells, before and after the inside surfaces were painted.

I. SUMMARY

In order to study the structural response of a pressurized, reinforced concrete cell and evaluate its leaktightness, the cells (No. 4 and No. 5) of Building 315 intended to contain critical fast reactor experiments were pneumatically tested.

Each cell has the form of a rectangular box, with inside dimensions 30 x 40 x 30 ft high. To satisfy the requirements of biological shielding, the concrete thickness of exposed walls and ceiling is 4 ft. The thickness of the north wall, adjacent to the office building is 5 ft. The cells possess no special containment features, except that they are reinforced structurally with steel to withstand pressure loading from a large, sudden energy release and a subsequent internal static pressure. Construction was closely inspected but did not involve unusual methods. Although high-strength structural concrete (a minimum compressive strength of 4000 psi at 28 days) was specified and obtained, there were no special attempts to make the concrete leaktight.

The purposes of the structural tests were to investigate the ability of a cell to withstand static internal pressures at predictable stresses and strains, and to produce the basis for a future extrapolation of the behavior of the cell under dynamic loading. Leakage-rate tests were also conducted to determine the capability of the thick concrete walls and ceiling to retain air under pressure.

The strains in the walls and ceiling of Cell No. 5 were recorded with 39 SR-4 strain gages strategically placed on reinforcing steel. Strains were recorded for internal pressures of 2, 4, 6, 8, and 10 psig. These strains were subsequently compared with the strains determined by elastic analysis. The analytical stresses and strains were calculated for a homogeneous and isotropic linearly elastic material. The analysis involved typical 1-ft wide longitudinal and transverse frame bents and a rectangular box frame. Extremely close agreement was obtained for the majority of the locations. There is an apparent disagreement between analytical and experimental results in the vicinity of re-entrant corners and near the discontinuities of the doors. Most of these discrepancies are alleviated by application of the proper stress-concentration factors to the analytical results. Table I summarizes the comparative results without including correction for stress concentrations. The general pattern of cell behavior at 10 psig, as summarized in Table I, is shown in Figs. 10, 11, and 12.

Although no emphasis was placed on exclusion of leaks, it was decided to conduct experiments to locate and plug detectable leaks where possible, and finally to attempt leakage-rate testing. By this procedure it was hoped to gain general information with respect to the resistance to permeation of ordinary concrete construction by contained gases. Leaks were located by pressurizing the enclosure and applying soap solution on suspect areas. Initial attempts to plug leaks were made with some success. Thereafter, the cell was pressurized to 10 psig and a preliminary observation of the rate of pressure decay made. After several such attempts, it became obvious that the porosity of the concrete and lack of good sealing around door frames and other penetrations allowed leakage amounting to several percent of the contained gas per hour. This leakage rate was later materially reduced by painting the inside surfaces of the cells with a "nonporous" paint.

II. DESCRIPTION OF THE FACILITY

The structure under consideration is primarily the concrete containment cells No. 4 and No. 5 constructed to house the Argonne Fast Critical Experiments. A finished cell has the shape of a rectangular box. Its internal nominal dimensions are: length 40 ft, width 30 ft, and height 30 ft. At all corners, except those adjacent to the floor, 16-in. bevels

have been provided in order to minimize stress concentrations. All walls and ceiling, except the north wall, are 4 ft thick. The north wall adjacent to Building D-315 is 5 ft thick. The wall thicknesses were imposed by the requirements of biological shielding. The walls and the ceiling were designed as two-way slabs. Each face of a slab is reinforced by No. 8 deformed reinforcing bars at 6-in. centers, running in both directions.

Figures 1, 2, and 3 show the twin cells No. 4 and No. 5 under construction. Each cell possesses a large, thick, steel service door on the

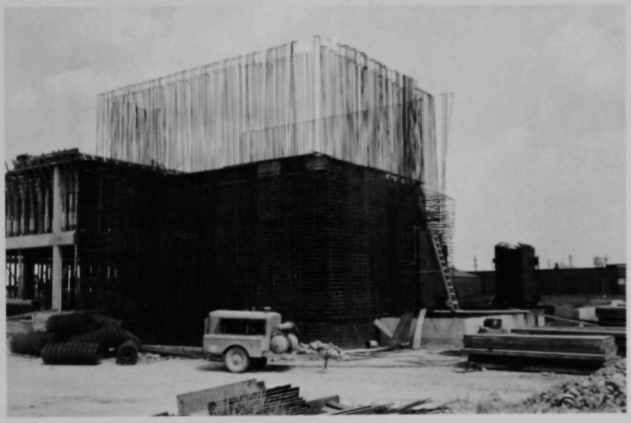

111-9529

Fig. 1. Containment Cell No. 5 during Placement of Reinforcement

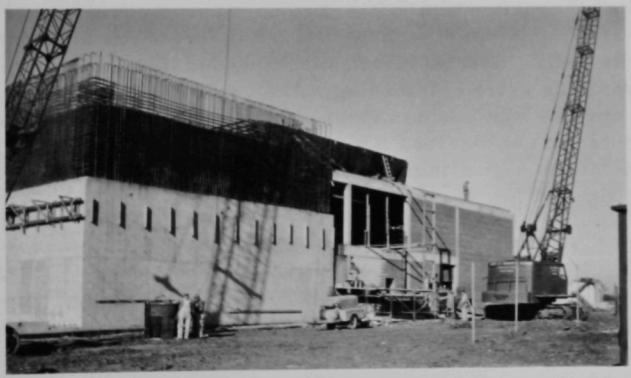

111-9989

Fig. 2. Completion of First Pour and Location of Construction Joint of Cell No. 4

111-9988

Fig. 3. Outside View of Completed Cell No. 5. To the Right, Twin Cell No. 4 under Construction

south wall and a smaller airlock door on the north wall connecting it to Building D-315. The only other important structural discontinuity is a large concrete well, extending to basement floor level in one corner, covered with removable precast slabs.

During construction an effort was made to employ techniques consistent with accepted good practice in the mixing, transportation, and placement of concrete. Concrete possessing a compressive strength of 4000 psi at 28 days was specified. To minimize possible planes of weakness originating at construction joints, two continuous pouring operations were employed, the only construction joint being located at approximately midheight of the walls. Special effort was expended to insure continuity at the joint by providing extra reinforcing. Also, prior to the second pour, the first joint surface was vacuum cleaned, wetted, and grouted. Subsequently, the tests did not disclose a plane of weakness resulting from the presence of the construction joint. Figure 3 shows the completed cell No. 5 and its twin cell No. 4 under construction.

III. PURPOSE OF TESTS

As in all containment vessels housing nuclear facilities, the aims of these tests were to acquire an insight into the behavior of the cells under pressure and to draw conclusions regarding performance under stipulated incidents. The cells were originally designed to withstand dynamic loads

resulting from a sudden energy release and a subsequent increase in internal static pressure. Actual full-scale blast tests in a nonexperimental facility such as these costly structures are, for obvious reasons, normally neither practicable nor customary. Any tests which must be conducted on the structure itself must be of such a nature as not to cause serious damage or otherwise to impair its future usefulness.

A. Purpose of Structural Pressure Tests

The structural tests were conducted in Cell No. 5 only. The reasons for pressure testing the cell at 2, 4, 6, 8, and 10 psig were primarily:

1. To observe and compare experimental with analytical strains and stresses, and to determine the validity of the static analysis, that is, to determine the ability of the cell to sustain internal static pressures at predictable stresses and strains.

2. To proceed with an attempt to extrapolate the performance of the cell under dynamic loads, if a satisfactory agreement is obtained between analytical and experimental results.

As a byproduct, these tests could also offer results of general interest in the field of structural mechanics. These aspects involve:

1. Subjecting a full-scale structure to perfectly distributed loading (pneumatic pressure) and observing its performance.

2. Providing an opportunity to the practicing engineer to compare his everyday methods of analysis with test results on full-size heavy frames and slabs. Heavy frames are common in the construction of bridges, viaducts, and heavy buildings. Experimental treatment, however, of such heavy structures is practically nonexistent.

B. Purpose of Leak-rate Testing

The leak-rate test was an experiment conducted in the cells to explore the capabilities of a reinforced concrete structure of this type to contain gases under pressure. Hope for success in this experiment was chiefly based on the massiveness of the cell walls and the rather meticulous care exercised during placement of the concrete to insure high strength and high density. In other respects, these cells were designed and constructed in the conventional manner. It was necessary, of course, to conduct preliminary pressure tests to detect and locate areas of gross leakage prior to a measured leakage-rate test, and to take such measures as seemed reasonable and practicable to eliminate or minimize such leaks.

IV. PRESSURE TESTS

For a successful performance of the pressure tests, a relatively leak-free cell was necessary. Prior to pressurization, considerable effort was expended to locate probable points of leakage and apply various techniques for sealing the leaks. After these general modifications, air was pumped into the cell with a large compressor, and several dry runs at pressures ranging up to 5 psig were performed. These allowed detection and repair of remaining leaks, and insured the adequacy of the pressurization equipment employed.

The first set of strain readings were taken at atmospheric pressure. This constituted the 0-psig reading. Subsequently, the pressure was increased in steps of 2 psi, and a set of strain readings were obtained at each step. Thus, strain readings for pressures of 2, 4, 6, 8, and 10 psi were recorded. Strain readings at the same pressure levels were also taken during the depressurization process. This pressure cycle was repeated once. Thus, for each pressure level, except 10 psig, four sets of strain readings were obtained. This was done in order to observe the consistency of performance of the strain gages and to detect gage drifts and any plastic flow of the concrete.

A. Testing Limitations Imposed by the Structures

Most of the nuclear-containment vessels heretofore employed are steel-plate structures of cylindrical or spherical shapes. Their design and erection procedures are relatively well established. Close adherence to the requirements of the ASME Unfired Pressure Vessel Code lends the benefit of accumulated experience and predictable performance. Except for some areas of leak-rate testing, acceptance tests for these vessels are relatively standardized. In most cases, repairs can also be carried out easily to satisfy acceptance requirements.

Employment of a reinforced concrete structure as a containment vessel introduces additional problems. Reinforced concrete, unlike steel, is a nonhomogeneous material. It does not possess the relative isotropy and ductility of steel. Concrete is strong in compression and weak in tension. Steel reinforcement is primarily used to take tensile stresses beyond the tensile strength of the concrete.

All pressure testing had to be conducted well within the tensile strength of the concrete employed in order to avoid cracking. This differs from common structural practice in which some cracking of the concrete in tension is almost necessary to develop fully the tensile capabilities of the reinforcement and to attest to efficient design. Cracking of the cell was undesirable because it would have increased the leakage probabilities and would have invalidated the design approach, which was based on the

precept that the concrete resisted tension during testing. An area of concern was the plane at the construction joint located at midheight of the walls, between the two pours.

Concrete can develop a tensile stress[1] of the order of one-tenth of its compressive strength. It can sustain a greater tensile stress caused by bending than by direct tension. With these considerations in mind, computations were performed to develop safe limits of internal pressures for the series of tests. Thus the maximum of 10 psig for internal pressure was selected in order to maintain the tensile stresses in concrete well within safe limits.

B. Instrumentation

To record tensile and compressive strains in the walls and the ceiling, the reinforcing bars were left bare at strategic locations by proper box-outs, both on the inside and outside surfaces. SR-4 strain gages were used for all measurements. They had to be applied between the corrugations of the deformed bars. The arrangement of strain gages was such as to disclose the performance of a transverse rigid frame bent, a longitudinal rigid frame bent, and a horizontal rectangular rigid frame box at approximately midheight of the cell.

To minimize the pronounced effect of plastic flow, three switching and balancing units were used by three operators simultaneously to record strains (see Fig. 4).

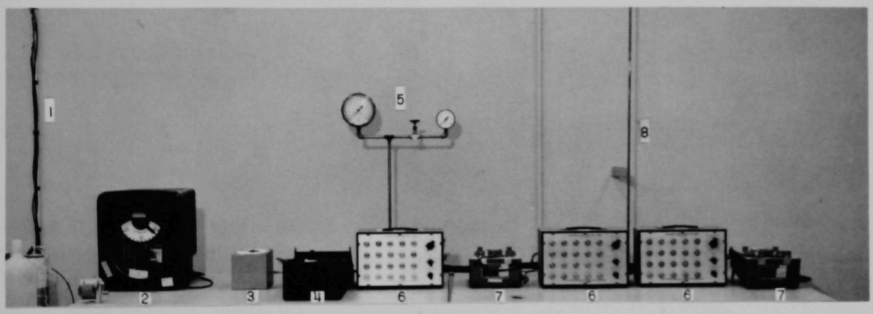

1. THERMOCOUPLE WIRES
2. ELECTRONIC DEW POINT RECORDER
3. WALL DEFLECTION INDICATOR
4. TYPE "K" STRAIN INDICATOR
5. PRESSURE GAGES
6. SWITCHING AND BALANCING UNIT
7. TYPE "N" STRAIN INDICATOR
8. WATER COLUMN

Fig. 4. Instrumentation Panel

The pressure in the cell during the tests was monitored by two pressure gages and a separate 30-ft water column connected to the cell and

extending from the basement through an opening in the first floor to the vicinity of the instrumentation panel. Both pressure gages and water column can be seen in Fig. 4.

C. Test Results

The experimental strains, in microinches, for the 2, 4, 6, 8, and 10 psig pressures are shown in Table I. The results were averaged for the two runs. The two runs provided four values for each of the 2, 4, 6, and 8 psig pressures and two values for the 10 psig pressures. Only those gage readings showing consistency for both runs were retained. The readings from one gage were discarded because it showed excessive drifts, indicating gage malfunction. Small drifts recorded at the end of each run were apportioned linearly to the recorded strains. In most cases, the gage drift was so small that it could not be apportioned in whole microinches to the various pressure levels. In these cases, in distributing whole microinches a larger proportion was allocated to the higher pressure levels (8 and 10 psig) to compensate for more active plastic flow of concrete at higher stresses.

D. Analytical Treatment

The cell was treated for moments, shears, stresses, and strains by analyzing a longitudinal frame bent, a transverse frame bent, and a rectangular box frame, (see Fig. 5). These frames represented

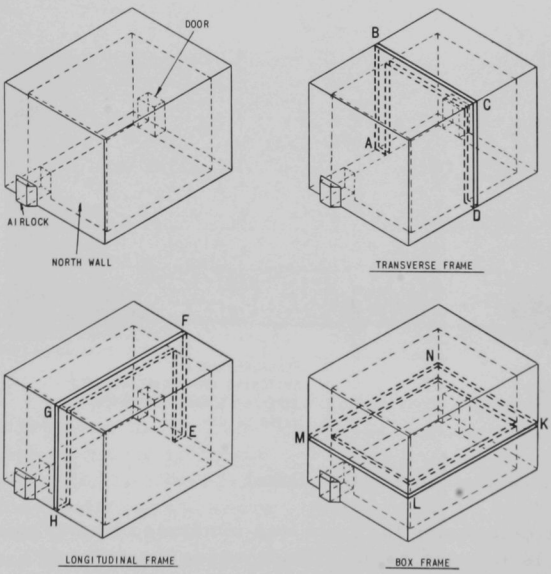

Fig. 5

Building Cell Showing Longitudinal and Transverse Frames and Rectangular Box Frame

Table I- COMPARISON OF ANALYTICAL AND EXPERIMENTAL STRAINS IN MICROINCHES
(NO STRESS CONCENTRATION EFFECT INCLUDED IN ANALYTICAL STRAINS)

PRESSURE / GAGE NO.*	1	2	3	4	5	6	7	9	11	13	14	16	17	18	19	20	21	22	23	24	25	26	27	28	29	30	31	32	33	34	35	36	38	39	40	41	42	43	44
2 PSI ANAL.	+4	-3	+2	-1	+5	-4	+2	-3	-1	+6	-5	-2	+6	-3	+4	-3	-4	+6	-2	+2	-4	+6	-3	+3	+4	-2	+1	0	+3	-2	+2	0	+2	-2	+3	-1	+3	-3	+4
2 PSI EXP	10	-4	3	-1	8	-6	9	-5	-3	7	-4	-4	5	-4	2	-4	-3	6	-4	3	-4	6	-3	4	5	-3	3	1	3	-2	7	0	3	-3	3	-2	3	-3	5
4 PSI ANAL.	+9	-5	+3	-3	+9	-7	+4	-7	-2	+12	-9	-4	+12	-7	+7	-5	-8	+12	-3	+5	-7	+13	-5	+7	+7	-4	+2	0	+6	-3	+4	-1	+5	-4	+6	-2	+5	-6	+8
4 PSI EXP	19	-7	5	-3	16	-10	14	-8	-6	12	-9	-4	11	-5	5	-6	-8	12	-3	5	-8	13	-5	8	7	-6	4	0	5	-4	14	0	7	-4	6	-2	6	-6	9
6 PSI ANAL.	+13	-8	+5	-4	+14	-11	+6	-10	-4	+18	-14	-7	+17	-10	+10	-8	-11	+18	-5	+7	-11	+19	-8	+10	+11	-6	+3	-1	+9	-5	+7	-1	+7	-6	+8	-3	+8	-8	+12
6 PSI EXP	30	-11	9	-5	24	-14	21	-12	-8	19	-11	-7	15	-6	7	-8	-11	20	-6	8	-14	22	-7	13	14	-5	8	-1	6	-6	19	0	12	7	10	-4	10	-6	15
8 PSI ANAL.	+18	-10	+6	-5	+19	-15	+8	-14	-5	+24	-18	-9	+23	-14	+14	-10	-15	+24	-6	+10	-15	+25	-10	+14	+14	-8	+4	-1	+13	-7	+9	-2	+10	-8	+11	-4	+10	-11	+15
8 PSI EXP	40	-14	12	-6	33	-19	28	-15	-10	26	-14	-9	19	-8	10	-10	-16	24	-7	10	-23	29	-9	14	17	-10	10	-1	8	-8	24	-2	15	7	13	-7	13	-9	19
10 PSI ANAL.	+22	-13	+8	-7	+24	-19	+10	-17	-6	+31	-23	-11	+29	-17	+18	-13	-19	+31	-8	+12	-18	+31	-13	+17	+18	-10	+5	-1	+16	-9	+11	-2	+12	-10	+14	-6	+13	-14	+19
10 PSI EXP	48	-17	15	-7	39	-23	32	-18	-11	32	-19	-11	23	-16	12	-13	-18	27	-9	12	-25	36	-11	16	23	-16	12	-1	14	-11	29	-2	15	20	14	-9	16	-12	20

* Gages numbered 8, 10, 12, 15, and 37 were defective.

hypothetical 1-ft-wide sections cut vertically or horizontally through walls and ceiling. The Moment Distribution Method[2] of analysis was used. A sample of computations is given in Appendix C.

The composite sections of steel and concrete were treated as homogeneous. The steel cross-sectional area of the reinforcement was transformed into equivalent concrete area. The resulting cross sections were treated as those of a homogeneous material, capable of sustaining tension and compression. Close inspection of the structure immediately after the pressure tests disclosed no visible cracks on the inside or outside surfaces, thus justifying the elastic design approach.

Moments, stresses, and strains were calculated for each point on the structure where a functioning strain gage was located (see Figs. 6 and 7). The stresses lying in the plane of a frame were designated by S_u, where

$$S_u = \frac{P_1}{A} \pm \frac{M_1 C}{I} \quad .$$

The stresses at right angles to the plane of a frame were designated by S_v, where

$$S_v = \frac{P_2}{A} \pm \frac{M_2 C}{I} \quad .$$

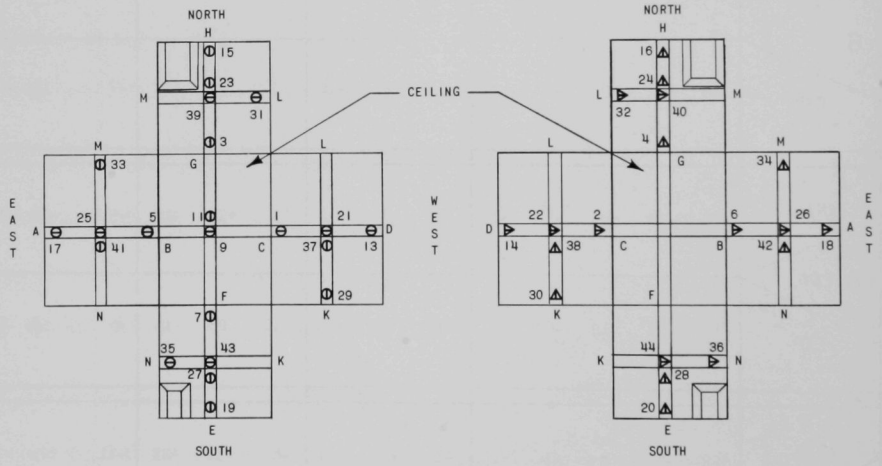

Interior Surfaces

Exterior Surfaces

Figs. 6 and 7. Arrangements of Strain Gages on Interior and Exterior Surfaces of Cell

Table II — GEOMETRIC PROPERTIES OF SECTIONS AND CALCULATED REACTIONS, MOMENTS, STRESSES, AND STRAINS FOR 10 PSIG PRESSURE

GAGE NO.*	1	2	3	4	5	6	7	9	11	13	14	16	17	18	19	20	21	22	23	24	25	26	27	28	29	30	31	32	33	34	35	36	38	39	40	41	42	43	44
	16,280	16,280	6,950	6,950	16,280	16,280	7,240	16,280	10,420	16,280	16,280	6,950	16,280	16,280	7,240	7,240	16,280	16,280	6,950	6,950	16,280	16,280	7,240	7,240	11,190	11,190	7,370	7,370	11,190	11,190	7,600	7,600	11,190	7,370	7,370	11,190	11,190	7,600	7,600
in.³	596.6	596.6	740.6	740.6	596.6	596.6	595.6	596.6	596.6	596.6	596.6	740.6	596.6	596.6	596.6	596.6	596.6	596.6	740.6	740.6	596.6	596.6	596.6	596.6	596.6	596.6	740.6	740.6	596.6	596.6	596.6	596.6	596.6	740.6	740.6	596.6	596.6	596.6	596.6
lb/in.²	27.3	27.3	9.4	9.4	27.3	27.3	12.1	27.3	17.5	27.3	27.3	9.4	27.3	27.3	12.1	12.1	27.3	27.3	9.4	9.4	27.3	27.3	12.1	12.1	18.8	18.8	10.0	10.0	18.8	18.8	12.7	12.7	18.8	10.0	10.0	18.8	18.8	12.7	12.7
³, lb-in.	+386	-445	+209	-300	+417	-582	+190.3	-622	-344	+582	-687	-450	+550	-550	+358	-358	-659	+665	-451	+455	-644	+673	-456	+452	+337	-318	+88.2	-110.0	+295	-282	+201	-105.2	+350	-515	+518	-347	+354	-481	+488
in.	20	20	26	26	20	20	20	20	20	20	20	26	20	20	20	20	20	20	26	26	20	20	20	20	20	20	26	26	20	20	20	20	20	26	26	20	20	20	20
in.⁴	118,400	118,400	229,350	229,350	118,400	118,400	118,400	118,400	118,400	118,400	118,400	229,350	118,400	118,400	118,400	118,400	118,400	118,400	229,350	229,350	118,400	118,400	118,400	118,400	118,400	118,400	229,350	229,350	118,400	118,400	118,400	118,400	118,400	229,350	229,350	118,400	118,400	118,400	118,400
in.³	5,920	5,920	8,820	8,820	5,920	5,920	5,920	5,920	5,920	5,920	5,920	8,820	5,920	5,920	5,920	5,920	5,920	5,920	8,820	8,820	5,920	5,920	5,920	5,920	5,920	5,920	8,820	8,820	5,920	5,920	5,920	5,920	5,920	8,820	8,820	5,920	5,920	5,920	5,920
, lb/in.²	+65.2	-75.1	+23.6	-34.0	+70.4	-98.3	+32.1	-105.0	-58.1	+98.3	-116.0	-51.0	+92.9	-92.9	+60.4	-60.4	-111.3	+112.3	-51.1	+51.5	-108.7	+113.6	-77.0	+76.3	+56.9	-53.7	+10.0	-12.4	+49.8	-47.6	+33.9	-17.7	+59.1	-58.3	+58.7	-58.6	+59.7	-81.2	+82.4
$= \frac{P}{A} + \frac{M}{S}$, lb/in.²	92.5	—	33.0	—	97.7	—	44.2	—	—	125.6	—	—	120.2	—	72.5	—	—	139.6	—	60.9	—	140.9	—	88.4	75.7	—	20.0	—	68.6	—	46.6	—	77.9	—	68.7	—	78.5	—	95.1
$= \frac{P}{A} - \frac{M}{S}$, lb/in.²	—	47.8	—	24.6	—	71.0	—	77.7	40.6	—	88.7	41.6	—	65.6	—	48.3	84.0	—	41.7	—	81.4	—	64.9	—	—	34.9	—	2.4	—	28.8	—	5.0	—	48.3	—	39.8	—	68.5	—
, lb/in.²	+92.5	-47.8	+33.0	-24.6	+97.7	-71.0	+44.2	-77.7	-40.6	+125.6	-88.7	-41.6	+120.2	-65.6	+72.5	-48.3	-84.0	+139.6	-41.7	+60.9	-81.4	+140.9	-64.9	+88.4	+75.7	-34.9	+20.0	-2.4	+68.6	-28.8	+46.6	-5.0	+77.9	-48.3	+68.7	-39.8	+78.5	-68.5	+95.1
, lb	11,190	11,190	7,370	7,370	11,190	11,190	7,600	10,420	16,280	11,190	11,190	7,370	11,190	11,190	7,600	7,600	11,190	11,190	7,370	7,370	11,190	11,190	7,600	7,600	16,280	16,280	6,950	6,950	16,280	16,280	7,240	7,240	16,280	6,950	6,950	16,280	16,280	7,240	7,240
/A, lb/in.²	18.8	18.8	10.0	10.0	18.8	18.8	12.7	17.4	27.3	18.8	18.8	10.0	18.8	18.8	12.7	12.7	18.8	18.8	10.0	10.0	18.8	18.8	12.7	12.7	27.3	27.3	9.4	9.4	27.3	27.3	12.1	12.1	27.3	9.4	9.4	27.3	27.3	12.1	12.1
/10³, lb-in.	—	—	—	—	—	—	—	-346	-626	—	—	—	—	—	—	—	-368	+376	-515	+521	-360	+358	-491	+477	—	—	—	—	—	—	—	—	+682	-453	+461	-677	+661	-460	+454
/8, lb/in.²	—	—	—	—	—	—	—	-58.4	-105.7	—	—	—	—	—	—	—	-62.2	+63.5	-58.4	+59.1	-60.8	+60.5	-82.9	+80.6	—	—	—	—	—	—	—	—	+115.2	-51.4	+52.3	-114.4	+111.7	-77.7	+76.7
$= \frac{P'}{A} + \frac{M'}{S}$, lb/in.²	18.8	18.8	10.0	10.0	18.8	18.8	12.7	—	—	18.8	18.8	10.0	18.8	18.8	12.7	12.7	—	82.3	—	69.1	—	79.3	—	93.3	27.3	27.3	9.4	9.4	27.3	27.3	12.1	12.1	142.5	—	61.7	—	139.0	—	88.8
$= \frac{P'}{A} - \frac{M'}{S}$, lb/in.²	—	—	—	—	—	—	—	41.0	78.4	—	—	—	—	—	—	—	43.4	—	48.4	—	42.0	—	70.2	—	—	—	—	—	—	—	—	—	—	42.0	—	87.1	—	65.6	—
, lb/in.²	18.8	18.8	10.0	10.0	18.8	18.8	12.7	-41.0	-78.4	18.8	18.8	10.0	18.8	18.8	12.7	12.7	-43.4	82.3	-48.4	69.1	-42.0	79.3	-70.2	93.3	27.3	27.3	9.4	9.4	27.3	27.3	12.1	12.1	142.5	-42.0	61.7	-87.1	139.0	-65.6	88.8
† $\mu\varepsilon_v$	3.8	3.8	2.0	2.0	3.8	3.8	2.5	-8.2	-15.7	3.8	3.8	2.0	3.8	3.8	2.5	2.5	-8.7	16.5	-9.7	13.8	-8.4	15.9	-14.0	18.7	5.5	5.5	1.9	1.9	5.5	5.5	2.4	2.4	28.5	-8.4	12.3	-17.4	27.8	-13.1	17.8
$\mu\varepsilon_u - \mu\varepsilon_v$	+88.7	-51.6	+31.0	-26.6	+93.9	-74.8	+41.7	-69.5	-24.9	+121.8	-92.5	-43.6	+116.4	-69.4	+70.0	-50.8	-75.3	+123.1	-32.0	+47.1	-73.4	+125.0	-50.9	+69.7	+70.2	-40.4	+18.1	-4.3	+63.1	-34.3	+44.2	-7.4	+49.4	-39.9	+56.4	-22.4	+50.7	-55.4	+77.3
$\varepsilon_u = \frac{1}{E}\ddagger(\varepsilon_u - \mu\varepsilon_v)$	+22.2	-12.9	+7.8	-6.7	+23.5	-18.7	+10.4	-17.4	-6.2	+30.5	-23.1	-10.9	+29.1	-17.4	+17.5	-12.7	-18.8	+30.8	-8.0	+11.8	-18.4	+31.3	-12.7	+17.4	+17.6	-10.1	+4.5	-1.1	+15.8	-8.6	+11.1	-1.9	+12.4	-10.0	+14.1	-5.6	+12.7	-13.9	+19.3

* Gages numbered 8, 10, 12, 15, and 37 were defective.

† $\mu = 0.20$

‡ $E = 4 \times 10^6$

E. Comparison of Analytical and Test Results

Of 44 strain gages employed, 5 proved defective and were ignored. Of these five, gages No. 10 and 12 were abandoned at the early stages of instrumentation due to moisture interference. Gages No. 8 and 37 were abandoned during the final check prior to the pressure tests. Readings from gage No. 15 were discarded during the progress of the tests due to general inconsistency and large drifts.

Of the remaining total of 39 gages that functioned properly, more than half, a total of 21, at the pressure of 10 psig, showed a maximum variation between analytical and experimental strains of zero to 3 μin., (see Table I). This would indicate accuracy far better than the accepted 10-μin. minimum error that is usually expected in strain-gage measurements.[3] For the remaining strain gages, the analytical results shown in Table I include no corrections for stress concentrations nor for discontinuities in the walls due to the service door and the airlock.

Figure 10 shows the proximity of gages No. 1, 3, 5, and 7 to the beveled corners between walls and ceiling. If a stress-concentration factor[4] of 1.88 is applied to the analytical strains of gage No. 1 (see Fig. 9), a closer agreement in the results is obtained. As can be seen in Fig. 9, the experimental results for gage No. 1, which is typical in the family of inside corner gages, are self-consistent, and exhibit almost perfect elastic behavior, lying on a straight line with an apparent stress-concentration factor of 2.18. It is suspected that the difference between the recommended factor of 1.88 and the apparent factor of 2.18 is due to the reduction of the wall thickness by 4 in. in order to reach the reinforcement, to the plastic flow of concrete at these comparatively highly stressed areas, and also to the dimensional inaccuracies that enter the analysis of very thick sections.

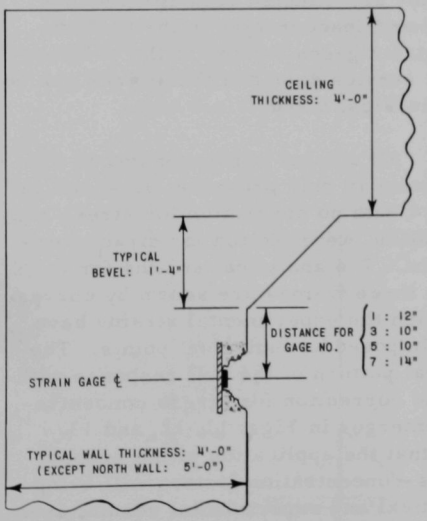

Fig. 10. Location of Gages No. 1, 3, 5, 7, Close to the Ceiling

Even among the results showing the greatest variation, consistency in the sign of strains prevails, with one exception. However, sensitivity of strain gages is illustrated in the

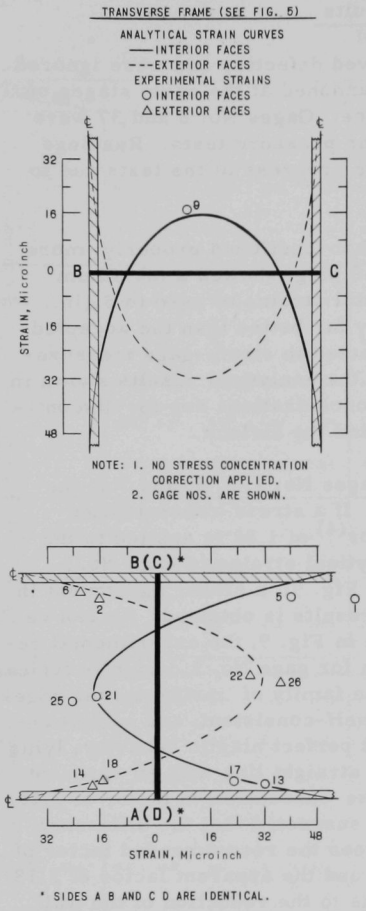

Fig. 11. Comparison of Analytical and Experimental Strains for Transverse Frame at 10 psig

unique case of gage No. 39. This gage, located very close to the corner of the airlock, was confronted with a stress pattern totally different than the one contemplated in the analysis. It is the only gage that recorded strains of opposite sign to those anticipated in the calculations. The wall cut out to permit entrance to the cell decreased the cross-sectional area participating in resisting the loads. Also, the proximity of gage No. 39 to the corner of the cut-out introduced stress concentration, resulting in a tensile instead of a compressive strain.

A comparison of the results for locations near the midspan of members shows satisfactory agreement (see Fig. 8). These areas are not subject to stress concentrations due to re-entrant corners, and they are affected very little by dimensional inaccuracies in the analysis. The strain gages located in the proximity of the service door and the airlock can be seen in Figs. 6 and 7.

All strains corresponding to the maximum 10 psig pressure, as shown in Table I with no correction for stress concentration, were plotted for direct comparison. The analytical strains for each of the three frames are shown by curves on which the experimental strains have been imposed as individual points. The general pattern of the cell response without the correction for stress concentration emerges in Figs. 11, 12, and 13. Note that the application of the proper stress-concentration factors will bring analytical and experimental results even closer.

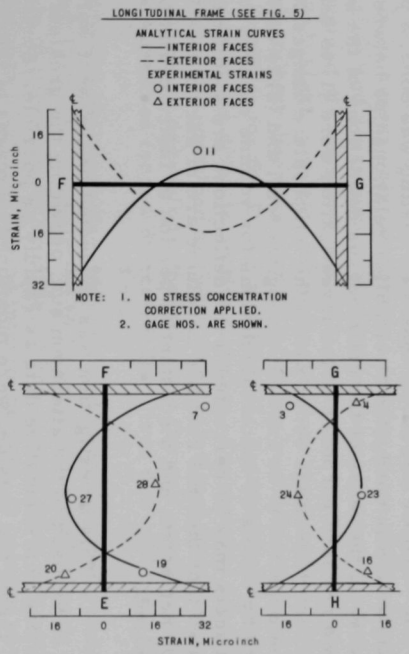

Fig. 12. Comparison of Analytical and Experimental Strains for Longitudinal Frame at 10 psig

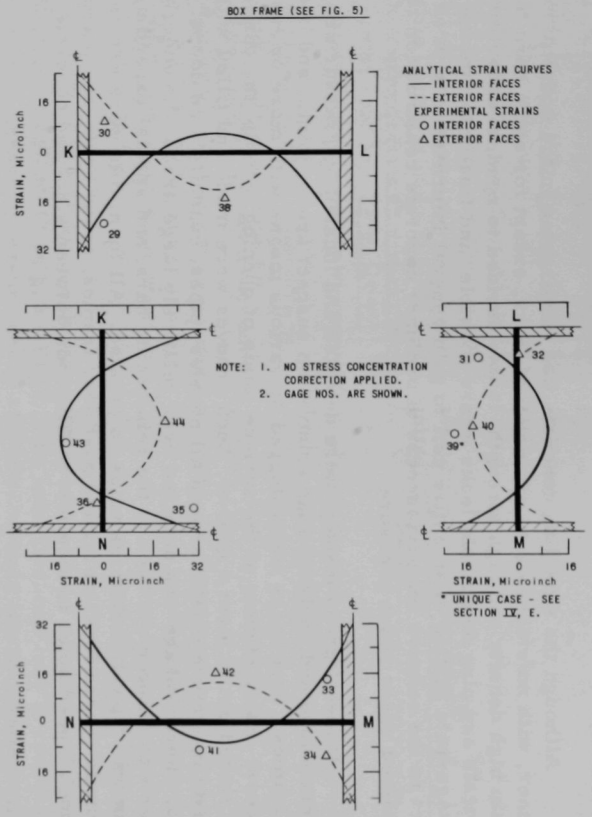

Fig. 13. Comparison of Analytical and Experimental Strains for Rectangular Box Frame at 10 psig

V. LEAK-RATE TESTING

A. General

Although the shielding concrete was constructed in the conventional manner, with no emphasis on exclusion of leaks, except for extra care to obtain high density and high strength, it was decided to conduct experiments to locate and plug detectable leaks where possible, and finally to attempt leakage-rate testing of an entire cell to gain general information with respect to the relative imperviousness of ordinary concrete construction to contained gases under pressure.

Areas of gross leakage were detected and located by pressurizing the enclosure and applying soap solution on suspect areas, joints, and opening frames. Such leaks were plugged by various means with more or less success. For instance, at the surface joints of opening frames, the concrete was routed out to form a groove. Such grooves were made and filled with a high-temperature mastic around all nozzles, pipes, conduits, and doors. Also, where leakage was detected over relatively large areas, the concrete cover was chipped out back to the reinforcing bars, and special expanding grout was trowelled into the voids so created. All form ties were carefully grouted. Where leaks persisted past door frames, epoxy resin was pumped through tapped holes in an effort to fill voids between steel and concrete.

B. Description of the Test

1. Before any actual leak-rate testing was done, a preliminary investigation was conducted to establish relationships between surface temperatures of the faces of the cells versus deflections of the inner surfaces. The two primary purposes of the investigation were (1) to determine whether significant deflections occur within the temperature ranges to which the cells may be expected to be exposed during the test; and (2) to establish experience factors by means of which calculations for volume changes due to temperature effects may be corrected if the deflections are significant. These tests indicated that thermal changes in volume are of such a small order that they may be neglected, and a substantial portion of instrumentation was thus eliminated.

This investigation was conducted on the west wall of Cell No. 5, which is exposed to the afternoon sun, providing the greatest contrasts for developing representative data as rapidly as possible. Surface temperatures, inside and outside, were monitored by means of thermocouples taped to the wall, and shaded and insulated with 6 x 6 x 1-in. blocks of wood taped over them. The location and number of thermocouples are shown in Fig. 14. The thermocouple readings were made with an indicating potentiometer of high accuracy. Deflections of the inner surface were measured at the center point of the wall by means of a dial gage mounted on tightly strung wires as shown in Fig. 15. Direct changes in length and height of the wall were neglected.

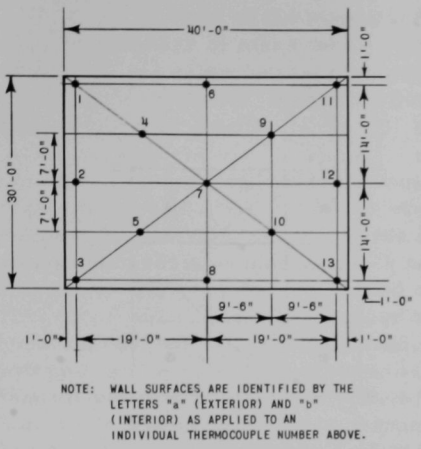

Fig. 14. Location of Thermocouples on Inner and Outer Surfaces of West Wall of Cell No. 5

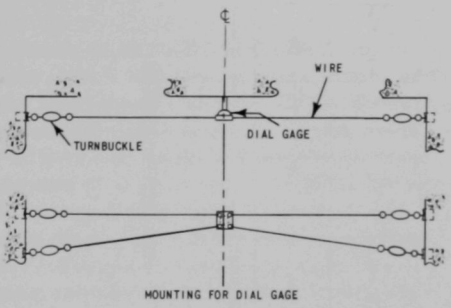

Fig. 15. Arrangement for Measuring Deflection at Center Point of Inside Surface of West Wall of Cell No. 5

2. The leakage-rate test proper was to have consisted of pressurizing a cell to 10 psig, sealing off the inlet line, and then over a sufficient period to observe pressure decay and contained air temperatures from which loss of air during any period could be calculated. Contained air temperatures were to be monitored by means of thermocouples suspended in the air space to obtain an average air temperature for any given observation. The number, location, and arrangement of the thermocouples are shown in Fig. 16. Contained air pressure was to be measured by means of a specially developed, highly accurate, absolute mercury manometer. Two of these instruments have been built by ANL for use in similar tests of the containment buildings for the EBWR and EBR-II. A complete description of these instruments is given in Section C below. Corrections for water-vapor pressure in the contained air were to be calculated from observations of either wet-bulb and dry-bulb temperatures in the cell, or dew point. The latter might be obtained from a direct-reading, true dew-point indicator.

When known leaks had been reduced to an expected practicable minimum, Cell No. 5 was pressurized to 10 psig, and a preliminary observation of the rate of pressure decay made. After several such attempts, with additional efforts to plug leaks during interim periods, it became obvious that the porosity of the concrete and lack of good sealing means around door frames and other penetrations allowed leakage amounting to several percent of the contained gas per hour.

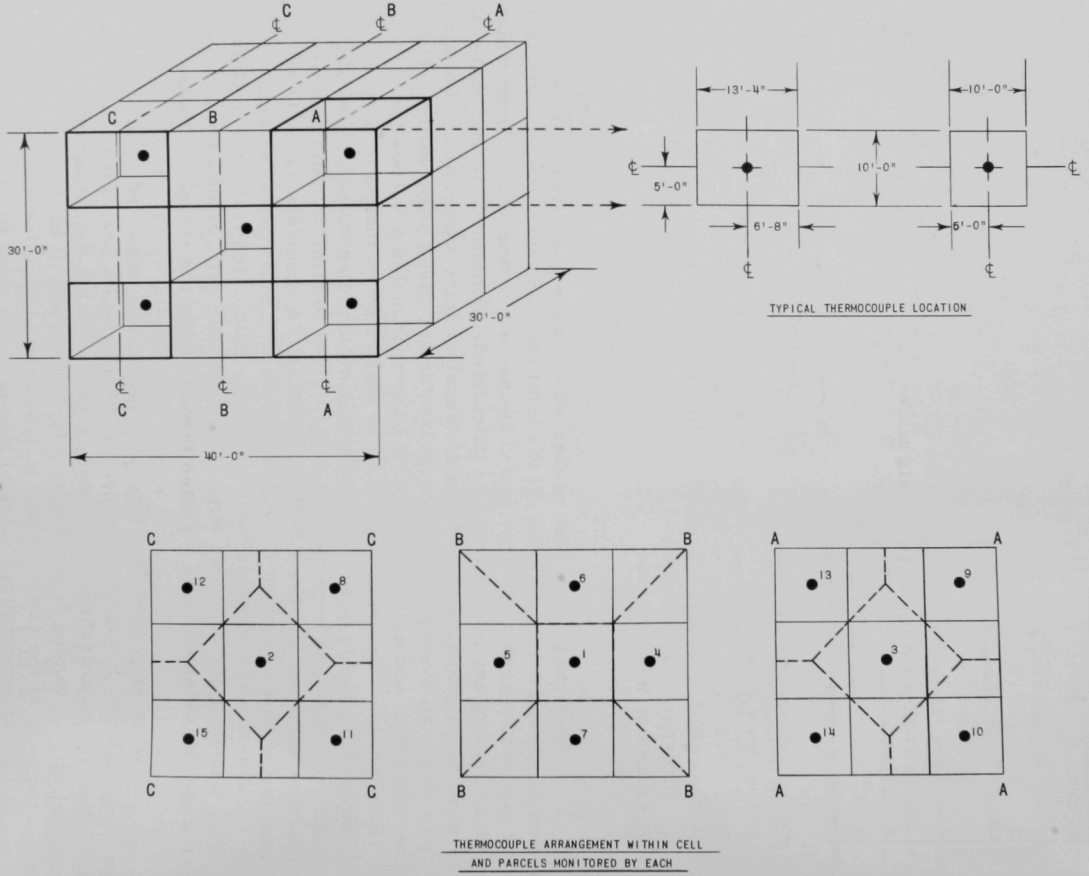

Fig. 16. Location of Thermocouples in Cell No. 5

In view of the magnitude of the leakage rate from Cell No. 5, it was unnecessary to make measurements with the accuracy originally planned. Hence, all instrumentation, thermocouples, etc., were dismantled and removed from the area. Pressure decay was measured on the water manometer without correction.

3. Following the foregoing attempts to perform a leakage-rate test, additional leak surveys of both cells (No. 4 and No. 5) were made, and further efforts made to plug known leaks and suspect areas. After these repairs, rough leak-rate tests at 10 psig showed a loss of ~23% of contained air per 24 hr from Cell No. 4, and of ~10% of contained air per 24 hr from Cell No. 5.[5] Since these leakage rates are still excessive, various means of lining the cells were considered, and it was finally decided to coat the interior of the walls with a phenolic resin-base paint to improve the capabilities for gas containment of both cells. The paint chosen was Carboline 305. When this interior painting was completed, additional pressure tests at 10 psig indicated reductions of leakage rates to about 8% per 24 hr for Cell No. 4 and to 6% per 24 hr for Cell No. 5.[6]

C. Instrumentation

1. Volume-change Effects due to Temperature Gradients through Walls

Wall-surface temperatures, inside and outside, were monitored by thermocouples as shown in Fig. 14. The deflections of the inner wall surface at the center were measured by a dial gage, as shown in Fig. 15.

2. Leakage-rate Test, Proper

The temperatures inside the cell during the leakage-rate test were to have been monitored by thermocouples suspended in the air space to provide readings for the calculation of the average air temperature. Their arrangement is shown in Fig. 16.

Pressure-sampling lines were tapped into closure plates on nozzles which are permanently sealed through a wall of the cell. Pressurization was accomplished via a similar nozzle and isolating valve. All instrument wiring and thermocouple leads were led through permanent conduits sealed through the cell floor and leading to the control room. The conductors were stripped at sealing condulets which were sealed off with epoxy resin.

3. Description of Absolute Manometer

Accuracy in pressure measurements beyond that attainable with commercially available equipment are usually required in cases where

leak rates are very small. An instrument was needed which could be read to the required accuracy by any of several operators. A description of the manometers evolved follows.

These manometers are designed for pressures up to 70 in. Hg abs for the EBWR tests and 90 in. Hg abs for the EBR-II tests. For ease of filling, the top (closed) end is sealed by means of a stopcock. Below the stopcock a glass capillary tube bent into a goose-neck is fused to the top of the main tube and the lower end of the stopcock. By pressurizing the mercury reservoir with argon or nitrogen, the mercury is forced up through the capillary and stopcock until it partially fills a small glass reservoir above the stopcock. The stopcock is then closed and sealed, and the gas pressure released slowly from the mercury reservoir.

The height of the mercury column is measured by means of a stainless steel rod cut accurately to a length about 12 in. short of the expected average pressure. Shorter rods cut accurately to length are used to extend this length to locate a sliding platform which clamps in place at 2-in. intervals. A micrometer height gage is clamped to this platform, and a reading sight is supported by this height gage by an accurately machined bracket. The height gage reads from 0 to 4 in.

A reading slot in the sight, which consists of a wide portion at the center and very thin portions at the sides, is accurately located. The meniscus is thus able to eclipse most of the aperture suddenly as its crest reaches the top of the slot (the tops of the three portions of the slot are coincident). A small, calibrated light bulb shines through the slot, and the intensity of the beam is sensed by a photoelectric cell at the opposite side. The signal from this cell is registered on a sensitive galvanometer which indicates the sudden near eclipse of the beam by a rapid fall of the pointer and gives a reading of the meniscus level of high precision.

To zero the lower end of the measuring rod, a sharp point is formed at its lower end. A low-voltage circuit induced through the reservoir wall and the rod, via an indicating red light bulb, is made or opened as the sharp point touches or leaves the surface of the mercury. The usual adjustable plunger immersed in the mercury is used to raise or lower the surface until the red light flickers out by light tapping on the reservoir.

These reading and zeroing means produce high accuracy and are repeatable to very close limits by almost any operator. Thus the human element is virtually eliminated from pressure measurement.

VI. CONCLUSIONS

A. Pressure Testing

1. Prior to the tests, it was advised that the expected strains to be recorded were so small that ordinary errors and instrument inaccuracies would overshadow the results and no distinguishable pattern would emerge. An important result of this investigation is that with sufficient care the accepted 10-μin. minimum error of instrumentation can be materially reduced.

2. The components of the cell made up of a nonhomogeneous and anisotropic material (concrete and steel) behave elastically in a predictable manner.

3. The elastic analysis of the heterogeneous material based on the uncracked sections is valid.

4. At re-entrant corners, the results of the elastic analysis must be modified by the proper stress-concentration factors.

5. With proper care during construction, construction joints can be made to sustain concrete tensile stresses at least as high as one-third of the tensile strength of concrete.

6. The negative moments along the edges of the slabs cannot be pinned down with certainty due to the necessary modification of the analytical results in these areas by empirical stress-concentration factors. Another source of error in the edge moments is the active plastic flow observed in these relatively high-stress areas.

B. Leak-rate Testing

1. Volume-change Effects due to Temperature Gradients through Walls

The range over which the difference between average inside surface temperature and average outside surface temperature on the west wall varied during approximately five weeks of observations was ~40°F. Based on deflection measurements at the center point of the inside surface of the wall, calculations, in which circular curvature and maximum free arc length were assumed, indicated a volume change of less than 0.01% over the full temperature range when applied to the three exposed walls and the roof of the cell simultaneously. This range of Δt is probably near the maximum that could be experienced within the period of a leakage test, especially for simultaneous variation in the exposed walls and roof. The value given above for ΔV is, therefore, probably greater than would be experienced.

This value is a small fraction of the error involved in measuring and calculating the volume losses. These volume-change effects due to temperature gradients through the cell structure were, therefore, considered negligible.

2. Leakage-rate Test, Proper

From the foregoing description and test results, it can be concluded that concrete enclosures, even where wall thicknesses are as great as 48 in. and 60 in., when constructed in the conventional manner, even though extra care is exercised to obtain high density and high strength, will leak excessively through inherent porosity, cracks, and crevices between steel frames and penetrations and the adjacent concrete. This appears to be true after considerable effort to improve conditions at joints between steel frames and penetrations and the concrete, and faults in local areas. Application of a good, nonporous paint to the inner surfaces reduces the leakage by a factor of ~2 to 3; but the leakage rate from the standpoint of containing radioactive gases may still be excessive.

Appendix A

INSTRUMENTATION PROCEDURE FOR STRUCTURAL PRESSURE TESTS

The instrumentation procedure had to comply with the requirements to measure very small elongations in a concrete reinforcing bar, less than one hundred microinches per inch (MII). To those who are familiar with the limitations of measuring techniques with strain gages, it is obvious that one can easily lose 100 MII due to equipment peculiarities and other errors, if sufficient care is not taken to analyze the situation. Briefly stated, the problem in these tests was to record very small strains. All the possible sources of error had to be investigated and their magnitude determined. In this way, even if the magnitudes of some errors could not be reduced, at least they were to be accounted for in an intelligent interpretation of the results.

1. Strain-gage Selection and Installation

The selection of the strain gage was affected by both the overall physical structure to be tested and the immediate area in which the gage was to be placed. Some of the gage locations were located 30 ft from ground level on the face of outside walls. This made it difficult to install the gages and exposed them to weathering. Also, the reinforcing bars to which the gages were to be attached were recessed and only half exposed in box-outs of the concrete wall. A clamping force was required for the gages in the vertical position. If one or two gages were all that were involved, an inexpensive jig could have been devised. However, there were 44 gage locations, and all were to be applied in a reasonably short time. Usually, when a gage is cemented to a specimen, it can be horizontally oriented, and a weight set on top of the gage to supply the required clamping force during the drying interval. To make up for the vertical orientation of the gages, a thin paper-base gage was chosen, the cement was allowed to dry out fast, and a magnet with sufficient attraction was used to hold the gage fixed to the steel reinforcing bar. A very fast-drying adhesive was tried at first, but better results were obtained with a Duco household cement.

The problem of selecting the proper strain gage for the ribbed reinforcing bar was further aggravated by the limitation placed on its physical dimensions. They had to be confined between 0.8 cm x 0.4 cm or 0.6 cm x 0.6 cm. For gages within these dimensions, special equipment to remove the ribs was unnecessary.

Forty-four gage positions were to be instrumented. The number of temperature-compensating gages doubles the total number. The accuracy required, the availability of the gages at that time, and the cost involved indicated that a standard gage was preferable to a special gage. On the basis of this observation, an A-8 type SR-4 strain gage was selected.

For each active gage a compensating gage was installed. The compensating gages inside the cell were placed on slugs mounted on the same

box-outs as the corresponding active gages (see Fig. 17). This was possible because of the little variation in the air temperature inside the cell and the 4-ft thickness of the walls limiting heat conduction. On the outside surfaces, a similar installation did not prove satisfactory. Although the gages were insulated, and the box-outs were taped and isolated, the excessive heat conduction caused the thermocouples at box-outs Nos. 2 and 14 to record sizable temperature differences between reinforcing bar and slug. Subsequently, the slugs were moved and loosely attached directly on the respective reinforcing bars. Thermocouple readings were again recorded. The results are shown in Figs. 18 and 19. This step was taken in order to determine the most appropriate time interval, during a 24-hr period, to conduct the pressure tests.

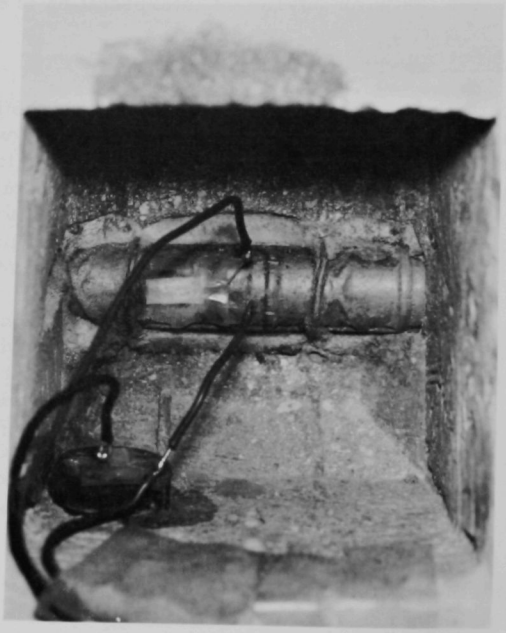

112-1125

Fig. 17. Arrangement Showing Strain Gage on Reinforcement with Compensating Gage on Slug

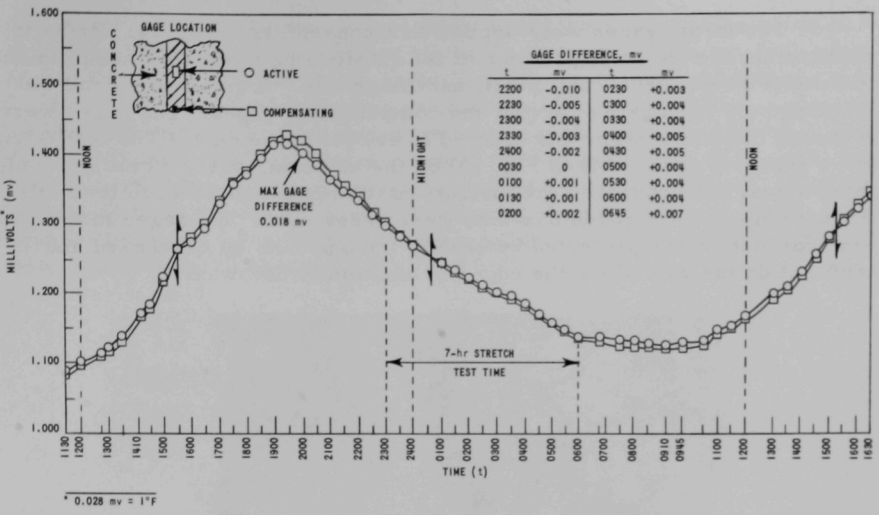

Fig. 18. Thermocouple Readings for Positions of Active and Compensating Gages at Port No. 2, to Establish Most Desirable Interval for Tests

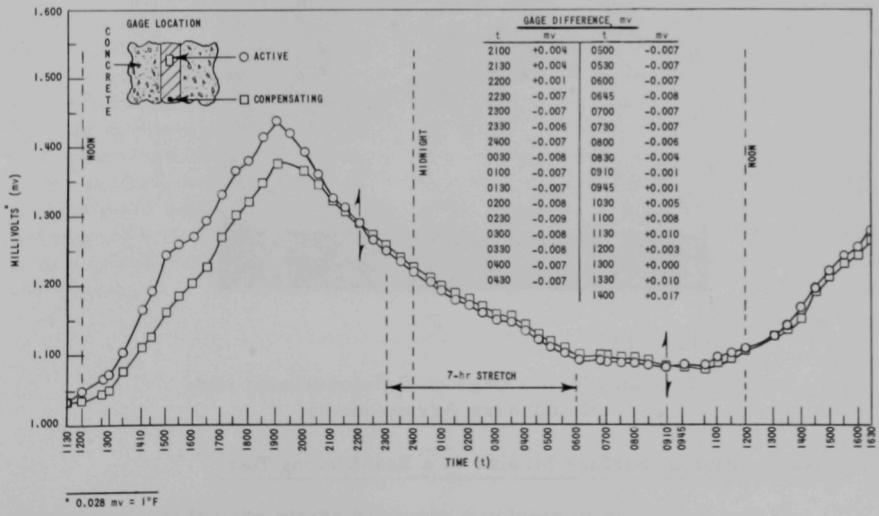

Fig. 19. Thermocouple Readings for Positions of Active and Compensating Gages at Port No. 14, to Establish Most Desirable Interval for Tests

The strain gages were applied in a conventional manner. Prior to application, the specific locations of the reinforcing bars were sand blasted to remove scale, dust, rust, paint, and/or grease. A three-wire lead was employed for each pair of active and compensating gages. The gages were trimmed of excess paper and allowed to dry for three days. The lead wires were securely attached (see Fig. 20) on the adjacent walls or ceiling, made into cables, and brought to the instrumentation panel adjacent to the cell. All the gages in the inside box-outs were beeswaxed. The gages in the outside box-outs were protected by sealing the box-outs by cardboard and taping it on the wall along the edges in addition to beeswax.

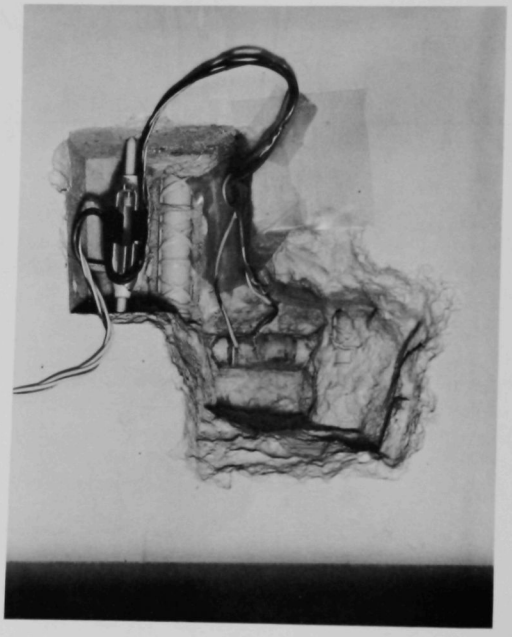

112-1124

Fig. 20. Strain Gage on Reinforcement with Lead Wire Arrangement

2. Investigation of Surface Strains in a Reinforcing Bar

It was desirable to employ a standard strain gage that was as long as possible. This condition would have brought the gage very close to the

rib of the reinforcing bar. The question arose - how close can the gage be to the rib without being perturbed by the rib? A test of the strain pattern in the area available for strain gage placement was made with stress coat. A photo, Fig. 21, of the result shows that at a very short distance from the rib the bar appears to have the characteristics of a rod without ribs. This fact indicated that a gage, located within the full geometric limitation, could be placed without special consideration of the rib effect. Had the rib effect been sufficiently pronounced to influence even the smallest of gages, a special device would have had to be built to remove the ribs and an additional cost added to the field testing.

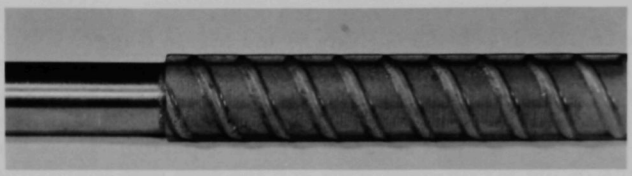

112-382

Fig. 21. Stress Coat for the Study of Surface Strains in Ribbed Reinforcing Bar

The surface of the specimen shown in the photo was first prepared by dressing it with a wire wheel. A magnaflux ST-2 thinner was then used to clean the surface. After the surface was freed of any lint, aluminum-pigmented lacquer ST-840 was sprayed at 20 psig pressure to provide a uniform background. Magnaflux coating ST-1205 was then sprayed at 12 psig to provide the brittle surface. The gas for both spraying operations was bottled dry nitrogen. The spraying temperature was 75°F and 60°F, dry and wet bulb, respectively; drying temperature was 80°F; testing temperature was 70°F. Crack initiation at approximately 800 MII was in agreement with the value supplied by the manufacturer. A dye was applied before photographing so that a visible residue would more clearly indicate the cracks.

Appendix B

ANALYSIS OF STRAIN-GAGE ERRORS

After the proper selection and installation of a strain gage, the various errors that could influence the experimental results were considered. These involve errors inherent in the manufacture and specifications of the gages, errors due to temperature fluctuations, and errors in the recording instruments and in over-all installation. These various sources of error are subsequently discussed independently and the magnitudes of their effects ascertained.

1. Error due to Transverse Sensitivity of the Strain Gage

In addition to measuring strain in a direction parallel to the axis of the strain gage, the gage also measures a fraction of the transverse strain due to Poisson's ratio. This fraction is dependent of the electrical characteristics of the strain-gage wire and the fact that approximately 4 percent of this wire is oriented in the transverse direction. To correct for this condition, the manufacturer supplies a gage factor that is calibrated with use of a material with a Poisson's ratio of $\mu_0 = 0.285$.

The equation that corrects for the situation of not having a material with $\mu_0 = 0.285$ is given by Murry[7] as follows:

$$\epsilon_x = \frac{\Delta R/R}{G.F.} \quad \frac{(1 - 0.285\ K)}{1 - \mu K} \quad ,$$

where

ϵ_x = strain in the axial direction

$\Delta R/R$ = fractional change in strain-gage resistance

G.F. = gage factor.

Values of K are given by Hetenyi.[8] The K value is an experimentally determined quantity that corrects for transverse sensitivity and is different for each gage. This effect was practically zero in the case of the Sr-4, A-8 gage. A -0.05% error would have occurred if μ were 0.260 and +0.03% error if μ equaled 0.300.

2. Error due to Gage-factor Specification Allowance

The strain indicator detects the true strain only if the correct gage factor is used. If the dial indicator is not set for the gage factor of the gage, the true strain is in error by the ratio of the indicated gage factor recommended by the manufacturer on the package to the actual gage factor

of the gage being used, that is,

$$\text{True strain} = (\text{indicated strain}) \times \frac{\text{indicated gage factor}}{\text{actual gage factor}} .$$

The manufacturer gave a possible ±2 percent allowance for the gage factor of the gage used; therefore, a possible error of ±2 percent could have been introduced into the true strain because each gage could not be checked for its gage factor. This error is inherent in the gage and could not be accounted for.

3. Error due to Misplacement of Gage from Axial Direction

The gages were placed on the cylindrical concrete reinforcing rod without the aid of mechanical positioning. An instrument of this type is sometimes used to align a strain gage perfectly. Without such a device, some misalignment is unavoidable.

From a small sampling of manual placements of gages, it was estimated that a reasonable maximum angular misplacement of 5° could be expected. A misplacement of this magnitude for an actual strain of 100 MII was found to be in error by only 0.76 MII. The strain error for such a small angle was approximated by assuming that the diagram in Fig. 22 was representative of the physical system.

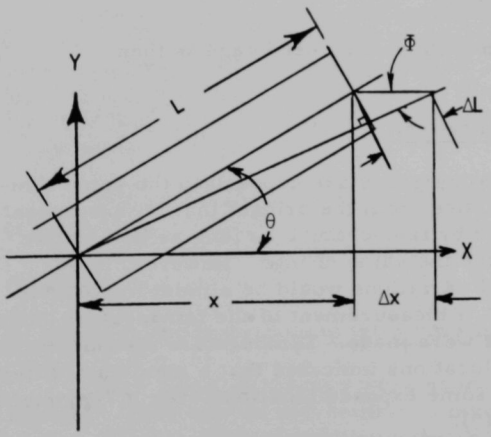

Fig. 22

Diagram for Error due to a Misplaced Strain Gage

The true strain is represented by

$$\epsilon_x = \frac{\Delta x}{x} ,$$

and the actual strain seen by the gage misplaced θ degrees is given by

$$\epsilon_\theta = \frac{\Delta L}{L} \quad ,$$

where

$$L = x/\cos\theta$$

and

$$\Delta L = \Delta x \cos\theta \simeq \Delta x \cos\theta \quad ,$$

which results in

$$\epsilon_\theta = \frac{\Delta L}{L} = \frac{\Delta x}{x} \cos^2\theta$$

or

$$\epsilon_\theta = \epsilon_x \cos^2\theta \quad .$$

The result is that the error ϵ_e is given by the relationship

$$\epsilon_e = \epsilon_x - \epsilon_\theta = \epsilon_x (1 - \cos^2\theta) \quad ,$$

and the fractional error due to an axially misplaced gage is then $\epsilon_e/\epsilon_x = \sin^2\theta$.

4. Error in Temperature Compensation

When active and compensating gages are exposed to the same temperature, there is no strain indication from the bridge; that is, a temperature-compensation circuit is unaffected by temperature as long as both active and compensating gages experience the same change. However, to be completely free from any thermal variations would be almost impossible in a field installation. Therefore, a measurement of the temperature variations at the locations of the gages were made. Temperature measurements of active and compensating gage locations indicated that a maximum difference of $\frac{1}{3}^\circ$F could be expected in some exposed locations over a 7-hr night testing period (see Figs. 18 and 19).

Temperature compensation of active and compensating strain gages is composed of two factors. First, the resistance of the gage wires change with temperature, and, second, the thermal coefficient of expansion of the strain gage differs from that of the structure on which it is bonded. To evaluate these small temperature changes, strain gages were affixed to

samples of the reinforcing bar used in the construction of the cell. Temperatures of the active and compensating gages were then changed in separate enclosures that were isolated and insulated. The change in apparent strain versus the change in temperature was a straight-line relationship with a slope of +4.5 MII/°F. This variation made obvious the necessity of night testing, because it represented a large error for the small strain readings recorded. Some locations had maximum readings of about 40 MII. The $\frac{1}{3}$°F temperature variation meant that this error for the larger strain readings could amount to a maximum of 4% and to a greater percentage for the smaller strains.

5. Error due to Lead Wires

In general, strain-gage lead wires are thick, single-stranded electric conductors with a good quality of insulation. The diameter of the wire should be as large as practicable in order to offer the least possible resistance to the passing current. By use of a temperature-compensating circuit, consistent changes in all lead-wire resistances due to consistent temperature changes in all wires do not affect the strain readings of the gages. The common lead is in the battery circuit and may be at a slightly different resistance than the other two leads. This fact is helpful in choosing the best possible combination of leads, that is, if there is a lead considerably different than the others that must be utilized, it would be wise to use it as the common lead.

Some rough handling was expected in the installation of the lead wires, and therefore, a test was devised so as to indicate what error could have been expected from this treatment. Twenty-five 180° bends were made in a 100-ft length of lead wire. The wire was straightened, and a check of the change of wire resistance due to cold working was not measurable.

The route that some of these leads took brought them to the outside of the building. Therefore, a careful layout was made to assure that no mechanical strain could affect the lead wires and the resulting strain readings.

6. Error in the Operation of the Switching Unit

Very small responses were expected from the active strain gages. This fact alone was an inducement to investigate every possible source of error. When a check of the switching and balancing unit was made, it was found that the repeated readings were not sufficiently accurate for the small ranges involved. A typical response of the switch selection, No. 6, on the switching unit (as received from the factory) is shown on the bar chart of Fig. 23a. An examination of the switch inserts was made in an attempt to correct this condition. The case was not dust proof and something

resembling a lubricant was observed on the switch contacts. After cleaning the switch, it was observed that a slight tapping did seat the switch better and gave readings represented by Fig. 23b.

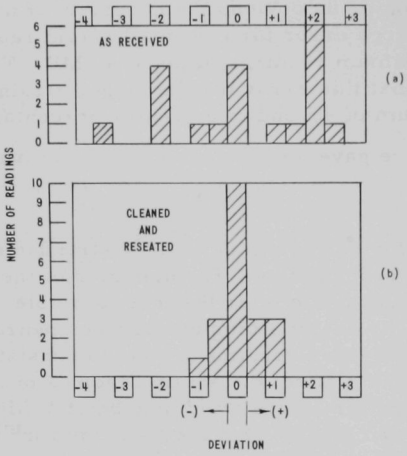

Fig. 23

Strain Gage Error due to Switching Unit

Other switch selections were similar to position No. 6. This selection was chosen at random to be representative of the switching boxes.

The probable error due to a single observation after cleaning was less than one percent of the expected strain and was acceptable considering the other errors.

7. Zero-drift Error

Instead of trying to stop the strain-indication instruments from drifting, a reference circuit was used wherein a known condition of zero strain existed. Once the system was balanced, any strain registered by the reference circuit was accepted as drift in the strain indicator. The field readings were then adjusted by this amount to acquire the corrected strain reading.

Appendix C

TYPICAL ANALYSIS FOR STRAINS

For purposes of illustration, the strains of gage No. 18 are considered. The analytical strains were calculated by Hooke's Law:

$$\epsilon = \frac{1}{E}\left(\frac{P}{A} \pm \frac{Mc}{I} - \mu\, S_v\right) \quad .$$

The 10 psig internal pressure gave a uniformly distributed load of 1440 lb/ft^2 acting on the inside surface of the structure. According to two-way slab theory,[9] based on equal deflection of the central strips, the (greater) portion of the load on a one-foot-wide strip of the wall is carried in the shorter of the two directions:

$$w_s = \frac{w\,L^4}{S^4 + L^4} = \frac{w\,(43.25)^4}{(33.33)^4 + (43.25)^4} = 0.740\ w$$

w_s = Portion of the total load w carried on the middle strip of the short direction of the east wall, i.e. portion of load acting on side AB of the frame in question.

L = long dimension of east wall

S = short dimension of east wall.

End moments resulting from the continuity of the structure were calculated by the Moment Distribution Method:[2]

FEM = Fixed End Moments

FEM_{AB} = 1/12 (w_s 30.5 ft*) 33.33 ft

= 1/12 (0.740 x 144 in.^{2}/ft^2 x 10 lb/in.^{2} x 30.5 ft) 33.33 ft

= 90,200 ft-lb = FEM_{BA}

FEM_{BC} = FEM_{CB} = 88,500 ft-lb

K = Moment Distribution Constant

$K_{BA} = \frac{I}{S} = \frac{118{,}400\ \text{in.}^4}{33.33\ \text{ft}} = 3{,}560\ \text{in.}^4/\text{ft}$

I = Moment of Inertia of 4-ft reinforced concrete wall

S = Effective length of wall.

*The actual clear height of the cell during the tests was 30.5 ft. After the tests, the final 6 in. of concrete was poured on the floor, reducing the height to 30 ft.

Similarly,

K_{BC} = 3,620 in.^{4}/ft

D = Moment Distribution Factor

$$D_{BA} = \frac{K_{BA}}{K_{BA} + K_{BC}} = \frac{3,560}{3,560 + 3,620} = 0.496$$

D_{BC} = 0.504

For all practical purposes,

$D_{BA} = D_{BC} = 0.5$

MOMENT DISTRIBUTION:

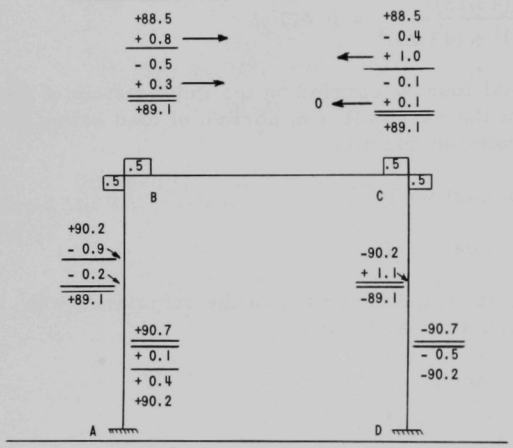

LOADING:

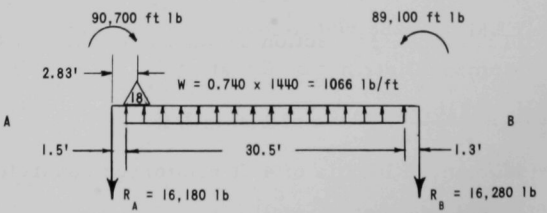

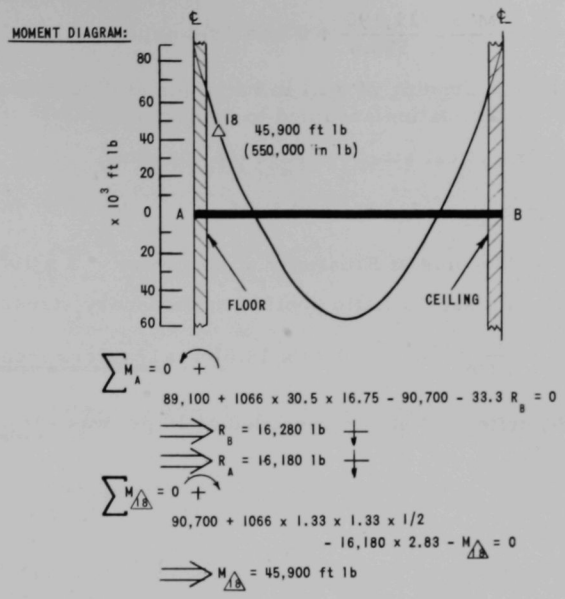

The Three Stress Components:

S_B = stress due to bending

$$S_B = \frac{Mc}{I} = \frac{550{,}000 \text{ in.-lb} \times (-20 \text{ in.})}{118{,}400 \text{ in.}^4} = -92.9 \text{ psi}$$

c = distance from neutral axis to strain gage locations

= -20 in.

S_P = tensile stress due to uplift of the ceiling

$$= \frac{P}{A} = \frac{16{,}280 \text{ lb}}{596.6 \text{ in.}^2} = 27.3 \text{ psi}$$

P = Uplift force on a section of wall, 1 ft wide and 4 ft deep

A = Equivalent concrete cross-sectional area

S_{18} = Stress in the direction of strain gage

$$= \frac{P}{A} \pm \frac{Mc}{I}$$

$$= S_u = 27.3 - 92.9 = -65.6 \text{ psi}$$

S_v = stress at right angles to the direction of the strain gage, i.e. tension in the longitudinal direction of the east wall.

$$S_v = \frac{P'}{A} \pm \frac{M'c}{I} = \frac{11{,}190}{596.6} + 0 = +18.8 \text{ psi}$$

M' = 0 bending of wall in longitudinal direction close to foundation assumed to be negligible.

$\epsilon_{\triangle 18}$ = Analytical strain at gage $\triangle 18$ location.

$$= \frac{1}{E}(S_{\triangle 18} - \mu S_v) \text{ by Hooke's Law}$$

E = Modulus of Elasticity of concrete, 4×10^6

μ = Poisson's Ratio applied to secondary stress, 0.20

$$\epsilon_{\triangle 18} = \frac{1}{4 \times 10^6}(-65.6 - 0.20 \times 18.8) = \underline{\underline{-17 \text{ micro inches}}}$$

The experimental strain recorded at 10 psi was $\underline{\underline{-16\mu \text{ in.}}}$

REFERENCES

1. G. E. Troxell and H. E. Davis, Composition and Properties of Concrete, McGraw-Hill Book Co., Inc., New York (1956), p. 177.

2. J. I. Parcel and R. B. B. Moorman, Analysis of Statically Indeterminate Structures, John Wiley and Sons, Inc., New York (1955), p. 239.

3. E. C. Clark and G. C. Hammond, Magnitudes of Strain Gage Error, Exptl. Mechanics, 2, 187 (June 1962).

4. R. J. Roark, Formulas for Stress and Strain, McGraw-Hill Book Co., Inc., New York (1954), p. 347.

5. Reactor Development Program Progress Report, December 1961, ANL-6485, p. 21.

6. Reactor Development Program Progress Report, March 1962, ANL-6544, p. 13.

7. W. M. Murry and P. K. Stein, Strain Gage Techniques, Massachusetts Institute of Technology, Cambridge, Mass. (1958).

8. M. Hetényi, Handbook of Experimental Stress Analysis, John Wiley and Sons, Inc., New York (1950), p. 174.

9. G. E. Large, Basic Reinforced Concrete Design, The Ronald Press Co., New York (1950), p. 185.

ACKNOWLEDGMENTS

The subject containment cells and the adjacent building D-315 were designed by the Architect-Engineer firm of Skidmore, Owings and Merrill, who, in turn, employed Professors N. M. Newmark and W. J. Hall of the University of Illinois as blast-design consultants. Mr. R. O. Brittan provided guidance during the conceptual stages of design and offered constructive criticism throughout the testing phase of this project.

Mr. F. C. Beyer was the Reactor Engineering Division representative during design, construction, and testing. His cooperation in assembling equipment and in overall personnel and contractor coordination are appreciated. Mr. J. A. Costello performed the second set of strain calculations and assisted in the preparation of some sections of this report.

The efforts of technicians H. F. Ludwig, C. J. Roop, F. L. Willis, F. F. Kodrick, and H. M. McCall in different phases of instrumentation and in recording the test data are acknowledged.

Finally, the authors believe, special acknowledgment is due to R. T. Purviance for the majority of the instrumentation effort, for coordinating the work of the other technicians, and for succeeding to obtain controlled laboratory-model accuracy on a full-scale exposed structure under adverse weather conditions and difficult access.